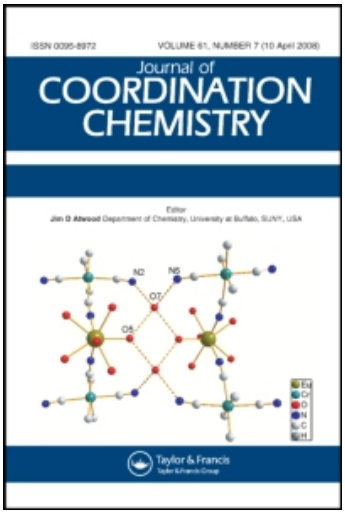

Journal of Coordination Chemistry
Publication details, including instructions for authors and subscription information:
http://www.informaworld.com/smpp/title~content=t713455674

Synthesis and characterization of a six-coordinate monomeric Mn(III) complex with SOD-like activity

Wei Shi[ab]; Yang Liu[ac]; Bin Liu[a]; Yuguang Song[a]; Yingkai Xu[a]; Hongmei Wang[a]; Yinlin Sha[c]; Guangzhi Xu[a]; Stenbjörn Styring[bd]; Ping Huang[b]
[a] State Key Laboratory for Structural Chemistry of Unstable and Stable Species, Centre for Molecular Science, Institute of Chemistry, Chinese Academy of Sciences, Beijing 100080, P.R. China [b] Department of Molecular Biomimetics, Uppsala University, S-75236 Uppsala, Sweden [c] Department of Biophysics, School of Basic Medical Sciences, Peking University, Beijing 100083, P.R. China [d] Department of Biochemistry, Centre for Chemistry and Chemical Engineering, Lund University, S-22100 Lund, Sweden

To cite this Article Shi, Wei , Liu, Yang , Liu, Bin , Song, Yuguang , Xu, Yingkai , Wang, Hongmei , Sha, Yinlin , Xu, Guangzhi , Styring, Stenbjörn and Huang, Ping(2006) 'Synthesis and characterization of a six-coordinate monomeric Mn(III) complex with SOD-like activity', Journal of Coordination Chemistry, 59: 2, 119 — 130
To link to this Article: DOI: 10.1080/00958970500249814
URL: http://dx.doi.org/10.1080/00958970500249814

Journal of Coordination Chemistry
Vol. 59, No. 2, January 2006, 119–130

Synthesis and characterization of a six-coordinate monomeric Mn(III) complex with SOD-like activity

WEI SHI†§, YANG LIU*†‡, BIN LIU†, YUGUANG SONG†, YINGKAI XU†, HONGMEI WANG†, YINLIN SHA‡, GUANGZHI XU†, STENBJÖRN STYRING§¶ and PING HUANG*§

†State Key Laboratory for Structural Chemistry of Unstable and Stable Species, Centre for Molecular Science, Institute of Chemistry, Chinese Academy of Sciences, Beijing 100080, P.R. China
‡Department of Biophysics, School of Basic Medical Sciences, Peking University, Beijing 100083, P.R. China
§Department of Molecular Biomimetics, Uppsala University, S-75236 Uppsala, Sweden
¶Department of Biochemistry, Centre for Chemistry and Chemical Engineering, Lund University, P.O. Box 124, S-22100 Lund, Sweden

(*Received in final form 28 February 2005*)

The complex $[Mn^{III}(HL)(L)(py)(CH_3OH)] \cdot CH_3OH$ (H_2L = 2-*ortho*-hydroxyphenylbenzimidazole, py = pyridine), **1**, has been characterized spectroscopically and by X-ray crystallography. The complex is triclinic, space group $P\bar{1}$ with $a = 10.396(2)$, $b = 10.7340(10)$, $c = 15.193(2)$ Å, $\alpha = 73.193(4)^\circ$, $\beta = 76.283(8)^\circ$, $\gamma = 61.400(40)^\circ$, $V = 1415.1(4)$ Å^3, $Z = 2$, $D_c = 1.445\,Mg\,m^{-3}$, $M_r = 615.56$, $\mu = 0.515\,mm^{-1}$, $F(000) = 640$, $R = 0.0631$, $wR = 0.1525$. Manganese is six-coordinate in an N_3O_3 ligand sphere created by two bidentate H_2L ligands and solvent molecules with a slightly distorted, axially elongated octahedral geometry. Electronic absorption spectra show π–π^* and Ligand Metal Charge Transfer (LMCT) transitions in the UV region and d–d transitions in the visible region. Solvent molecules coordinated to the Mn(III) ion in the crystal are thought to retain their coordination in solution. It is shown that **1** has reaction activity with the superoxide ion, as indicated by inhibition of pyrogallol autoxidation and by spin trapping electron paramagnetic resonance (EPR) spectroscopy. The N_3O_3 ligand set in **1** is similar to that in native MnSOD (superoxide dismutatase) in the substrate-bound state. The correlation between the ligand set in **1** and its reaction with the superoxide ion is discussed.

Keywords: Manganese(III); 2-*o*-Hydroxyphenylbenzimidazole; Pyridine; X-ray structure; Superoxide dismutase; Superoxide ion reactivity; 2,2-Dimethyl-3,4-dihydro-2*H*-pyrrole-1-oxide; Spin trap; Pyrogallol autoxidation

1. Introduction

Superoxide dismutase (SOD) is a group of ubiquitous metal-containing enzymes that catalyzes the dismutation of the superoxide radical anion, $O_2^{\bullet-}$, a damaging

*Corresponding author. Email: ping.huang@fki.uu.se; yliu@iccas.ac.cn

ISSN 0095-8972 print: ISSN 1029-0389 online © 2006 Taylor & Francis
DOI: 10.1080/00958970500249814

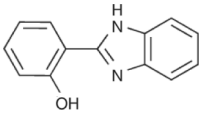

Scheme 1. Structure of H_2L.

physiological by-product, to molecular dioxygen and hydrogen peroxide. These enzymes serve a vital role in protecting oxygen-utilizing life from oxidative damage [1, 2]. Inadequate SOD levels lead to overproduction of radical by-products and hence to varies diseases. Studies of native SOD and SOD mimics have long served as guides for drug development, and synthetic complexes that possess SOD-like activity for potential pharmaceutical applications have been explored [3, 4].

The transition metals Cu, Zn, Fe, Ni and Mn are utilized in natural SOD enzymes [5–7]. Among synthetic complexes, however, Mn has been favoured [8] due to its inertness to the Fenton reaction that involves free metal ion reacting with hydrogen peroxide to generate hydroxyl radicals. Transition metals such as Fe and Cu in complexes often encountered in many SOD mimics have high Fenton reaction activity. Since hydrogen peroxide is one of the products of superoxide dismutation, synthetic complexes that contain Cu or Fe have high risk of toxicity as drug candidates, even though they may be good SOD mimics [9–14]. However, low molecular weight synthetic complexes are advantageous in terms of assimilability, an important consideration in drug design.

At the active site of native MnSOD, the Mn ion is five-coordinate with an N_3O_2 ligand set, with trigonal bipyramidal coordination geometry [15–18]. One of the ligands is a water molecule. It has been suggested that upon substrate binding the metal centre accommodates the substrate oxygen as the sixth ligand without displacing the coordinated water molecule [19]. Accordingly, a detailed reaction mechanism that involves alternation of coordination number and geometry of the metal centre in response to substrate binding and product dissociation during the catalytic cycle has been suggested [19]. Moreover, an extended hydrogen bond network on the outside of the first coordination sphere has been suggested to play an important role in controlling the enzyme's catalytic activity [20–22]. H-bonds also assemble the functional enzyme (dimers or tetramers) in native SOD. The hydrogen bond network is thought to aid mobility of protons that are involved in the dismutation, and thus to be essential for SOD function.

In this article, the synthesis and characterization of a monomeric manganese complex, $[Mn^{III}(HL)(L)(py)(CH_3OH)]\cdot CH_3OH$ (H_2L = 2-*ortho*-hydroxyphenylbenzimidazole (scheme 1), py = pyridine), **1**, is reported. We show that **1** possesses reaction activity with superoxide anion. The correlation between the ligand set in **1** and the SOD-like activity is discussed.

2. Experimental

2.1. *Materials and methods*

All experiments were carried out under ambient conditions. Pyrogallol, KO_2, DMPO (2,2-dimethyl-3,4-dihydro-2*H*-pyrrole-1-oxide) and $Mn(OAc)_2\cdot 4H_2O$ (from Aldrich)

were used as purchased. $N(n\text{-}Bu_4)MnO_4$ and H_2L were prepared as previously reported [23, 24]. All other chemicals of analytical grade were used without further purification. CAUTION: Appropriate care should be taken in the use of organic permanganates.

2.2. *[$Mn^{III}(HL_1)(L_1)(py)(CH_3OH)]\cdot CH_3OH$ (1)*

$Mn(OAc)_2\cdot 4H_2O$ (166 mg, 0.7 mmol) in 3 cm^3 of methanol was added to H_2L (409 mg, 1.9 mmol) in 8 cm^3 of pyridine. After mixing for 10 min, solid $N(n\text{-}Bu_4)MnO_4$ (97 mg, 0.27 mmol) was added in small portions during approximately 10 min. The resulting solution was stirred for 20 min at room temperature and then allowed to evaporate in air. Dark green crystals of **1** were obtained with 42.3% yield (based on $Mn(OAc)_2\cdot 4H_2O$). Melting point (m.p.) 230°C. Molecular empirical formula of **1**: Anal. Calcd for $C_{33}H_{30}MnN_5O_4$ (%): C, 64.33; H, 4.87; N, 11.37. Found: C, 64.41; H, 4.95; N, 11.35.

2.3. *X-ray crystallography*

Single crystals of **1** were selected and mounted on a Rigaku R-AXIS RAPID imaging plate diffractometer. Diffraction data were collected at 293 K with graphite-monochromated Mo-$K\alpha$ radiation ($\lambda = 0.7107$ Å). The detector swing angle was 5.00°. Readout was performed in the 0.100 mm pixel mode. Absorption corrections were applied by correlation of symmetry-equivalent reflections using the ABSOR program. Data reduction was performed using SHELX97 [25]. The structure was solved by direct methods and difference Fourier syntheses, and was refined on F^2 by full-matrix least-squares techniques using SHELXL97. Data collection and refinement parameters are listed in table 1. Crystallographic data for the structure have been deposited with the Cambridge Crystallographic Data Centre (CCDC) as supplementary publication number CCDC 200196. Copies of the data can be obtained free of charge on application to CCDC, 12 Union Road, Cambridge CB2 1EZ, UK (Tel: (+44) 1223-336-408; Fax: (+44) 1223-336-003; E-mail: deposit@ccdc.cam.ac.uk). Website link: www.ccdc.cam.ac.uk/data.request/cif.

2.4. *Spectroscopic measurements*

Electronic absorption spectra of complex **1** in dimethylsulfoxide (DMSO), methanol or a mixture of acetonitrile and dichloromethane were recorded on a Pharmacia Biotech Ultrospec-3000 spectrophotometer in the wavelength range 250–800 nm. Spectra of a solution containing the free ligand and a solution of the free ligand and pyridine at a mol ratio of 2 : 1 in DMSO were also taken for reference. The reaction of **1** with superoxide was determined through inhibition of pyrogallol autoxidation [26, 27] in the presence of **1**. Pyrogallol (1,2,3-benzenetriol) reacts with dioxygen to form several products that are electrochemically active and can be monitored, for example, at 318 nm. Superoxide is one of the intermediates and the method is used as an assay of SOD activity [26, 27]. Pyrogallol autoxidation was monitored through the absorption of a 0.9 μM pyrogallol solution at 318 nm on a Shimadzu UV-160 spectrophotometer at 25.0 ± 0.1°C. For measurements of inhibition of pyrogallol autoxidation,

Table 1. Crystallographic data for $[Mn^{III}(HL)(L)(py)(CH_3OH)]\cdot CH_3OH$ (**1**).

Empirical formula	$C_{33}H_{30}MnN_5O_4$
Formula weight	615.56
Crystal size (mm)	$0.46 \times 0.25 \times 0.08$
Crystal colour	Dark green
Crystal system	Triclinic
Space group	$P\bar{1}$
a (Å)	10.396(2)
b (Å)	10.7340(10)
c (Å)	15.193(2)
α (°)	73.193(4)
β (°)	76.283(8)
γ (°)	61.400(4)
V (Å^3)	1415.1(4)
Z	2
T (K)	293(2)
D_{calc} (g cm^{-3})	1.445
μ (mm^{-1})	0.515
$F(000)$	640
θ Range for data collection (°)	2.21–27.48
Reflections collected/unique	9243/6181
Completeness to $\theta = 27.48$ (%)	95.2
Data/restraints/parameters	6181/6/401
Goodness-of-fit on F^2	0.965
Final R indices: R; wR	0.0631; 0.1525
Largest difference peak and hole (e Å^{-3})	0.725; −0.724

a stock solution of **1** in dimethylformamide (DMF) was first prepared. A series of aqueous 0.9 μM pyrogallol solutions containing varying concentrations of **1** (0, 0.617, 1.234, 1.851, 3.085 and 4.319 μM) in Tris-HCl buffer (50 mM, pH 8.2) were then prepared for the measurements.

2.5. *Spin trapping electron paramagnetic resonance (EPR) spectroscopy*

KO_2 was used as the $O_2^{\bullet-}$ source. The highly active $O_2^{\bullet-}$ radicals were stabilized by the spin trap DMPO to form a spin adduct DMPO–$O_2^{\bullet-}$ that is relatively stable [28–31]. DMPO–$O_2^{\bullet-}$ possesses a characteristic electron paramagnetic resonance (EPR) spectrum. DMPO–$O_2^{\bullet-}$ was generated in a solution that was 14.1 μM in KO_2 and 1.5 mM in DMPO. Reaction activity of **1** with $O_2^{\bullet-}$ was then measured in three EPR samples where **1**, in varying concentrations, was first mixed with KO_2, followed by addition of DMPO after 2 s. The final concentrations of **1** were 1.5, 15 and 150 μM, while concentrations of KO_2 and DMPO were 14.1 μM and 1.5 mM, respectively. A series of solutions, 14.1 μM KO_2, 150 μM complex **1**, 14.1 μM KO_2 and 150 μM complex **1**, and 50 μM complex **1** and 1.5 mM DMPO were prepared separately as controls. To check the stability of the DMPO–$O_2^{\bullet-}$ spin adduct against reaction with **1**, a sample that was 14.1 μM KO_2 and 1.5 mM DMPO and into which **1** was added (150 μM) was also prepared. DMSO was the solvent in all EPR samples. EPR spectra were recorded on a Bruker X-band ESP300 spectrometer at room temperature. Spectrometer settings were modulation amplitude 0.05 mT, modulation frequency 100 kHz, microwave power 12.9 mW and microwave frequency 9.5 GHz.

3. Results and discussion

3.1. *Crystal structure*

The single-crystal X-ray structure shows that the Mn(III) ion in **1** is six-coordinate with a slightly distorted, axially elongated octahedral geometry. Selected bond lengths and angles are listed in table 2. Bond angles N(1)–Mn(1)–O(3) and O(2)–Mn(1)–O(3) deviate from 90° only by 0.59° and 0.23°, respectively, whereas N(3)–Mn(1)–N(5) and O(1)–Mn(1)–N(5) deviate from 90° by 1.51° and 2.27°, respectively (see table 2). Equatorial sites are occupied by two bidentate H_2L ligands and the two axial sites are oxygen and nitrogen from solvents methanol and pyridine (figure 1). The longer axial bond lengths, 2.288 Å for Mn(1)–N(5) and 2.358 Å for Mn(1)–O(3), compare to equatorial distances that range from 1.874 Å for Mn(1)–O(2) to 2.028 Å for Mn(1)–N(3), and are consistent with Jahn–Teller distorted, octahedral, high spin Mn(III). Similar configurations have been observed elsewhere [32]. One of the coordinated nitrogen atoms of H_2L, N(1), is deprotonated whereas the other, N(3), is not. The N(1)–Mn bond is expected to be shorter than the N(3)–Mn bond, in agreement with the present data [Mn–N(1), 1.981; Mn(1)–N(3), 2.028 Å]. The crystal structure of **1** shows N···H–N hydrogen bonds between two adjacent molecules of **1**, as indicated by dashed lines in figure 2 (N···H–N, 2.178 Å; angle, 157.95°). The nitrogen atoms involved in the H-bond network originate from deprotonated and neutral benzimidazol rings.

In **1**, two bidentate H_2L ligands stabilize Mn coordination. These, together with two solvent molecules (methanol and pyridine), create an octahedral N_3O_3 ligand field, in line with the intention to mimic the active site of native MnSOD. In native MnSOD,

Table 2. Selected bond lengths (Å) and angles (°) for **1**.

Bond lengths	
Mn(1)–O(1)	1.886(2)
Mn(1)–O(2)	1.874(2)
Mn(1)–N(1)	1.981(2)
Mn(1)–N(3)	2.028(2)
Mn(1)–N(5)	2.288(3)
Mn(1)–O(3)	2.358(3)
N···H–N[a]	2.178
Bond angles	
N(1)–Mn(1)–O(3)	90.59(10)
O(2)–Mn(1)–O(3)	90.23(10)
N(3)–Mn(1)–N(5)	88.49(10)
O(1)–Mn(1)–N(5)	92.27(10)
N(5)–Mn(1)–O(3)	176.83(9)
O(2)–Mn(1)–O(1)	176.21(10)
O(2)–Mn(1)–N(1)	87.40(10)
O(1)–Mn(1)–N(1)	92.03(10)
O(2)–Mn(1)–N(3)	92.91(10)
O(1)–Mn(1)–N(3)	87.61(10)
N(1)–Mn(1)–N(3)	179.28(10)
O(2)–Mn(1)–N(5)	91.49(10)
N(1)–Mn(1)–N(5)	92.15(10)
O(1)–Mn(1)–O(3)	86.03(10)
N(3)–Mn(1)–O(3)	88.77(10)
N···H–N[a]	157.95

[a]Intermolecular hydrogen bond.

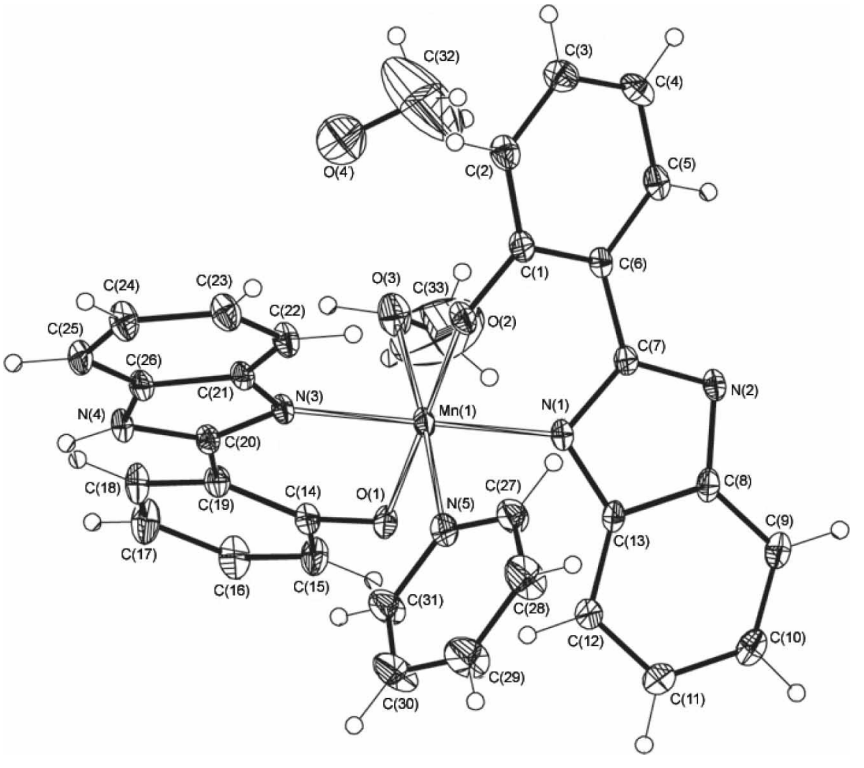

Figure 1. Molecular structure of complex **1** showing the atom labelling scheme.

as noted earlier, the manganese centre is five-coordinate, trigonal bipyramidal (N_3O_2) and, on substrate binding accommodates the incoming oxygen as the sixth ligand [19, 33]. Lah *et al.* [19] have suggested a reaction mechanism that involves alternating 5-6-5 coordination at the active site for FeSOD enzymes, though this is applicable to MnSOD as well. According to the proposal, the octahedral and trigonal bipyramidal geometries play important roles in the catalytic reaction. In a following section it is demonstrated that **1** shows reaction activity with superoxide. It is proposed that similarities to MnSOD in the ligand set and coordination arrangement in **1** is responsible for the SOD-like activity. Other six-coordinate Mn complexes that manifest similar SOD activity have been reported only in a few cases [34, 35].

3.2. *Electronic spectroscopy*

Figure 3 shows the electronic spectrum of **1** in DMSO. Change of solvent did not affect the spectrum. Table 3 lists absorption wavelengths and corresponding molar extinction coefficients for **1**, together with data for a mixture of free ligand and pyridine (at a molar ratio of 2 : 1) for comparison. In the UV region strong absorptions at 259, 291, 302, 317, 332 and a shoulder at 371 nm were observed for **1**. Bands at 259, 291, 317 and 332 nm are present in the spectrum of the free ligands, taking minor wavelength shifts into account. Accordingly, those bands can be attributed to π–π^* transitions of the ligand aromatic rings. It is noted, however, that absorption at 290 nm is much

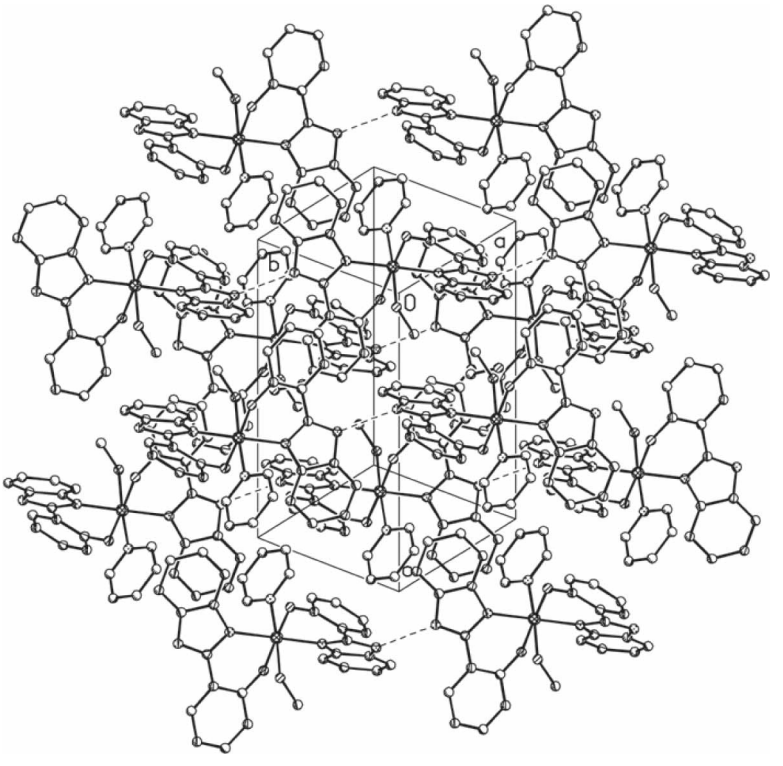

Figure 2. Molecular packing of **1**, viewed along the [111] direction. Dotted lines represent N–H···N H-bonds. Hydrogen atoms and solvent molecules are omitted for clarity.

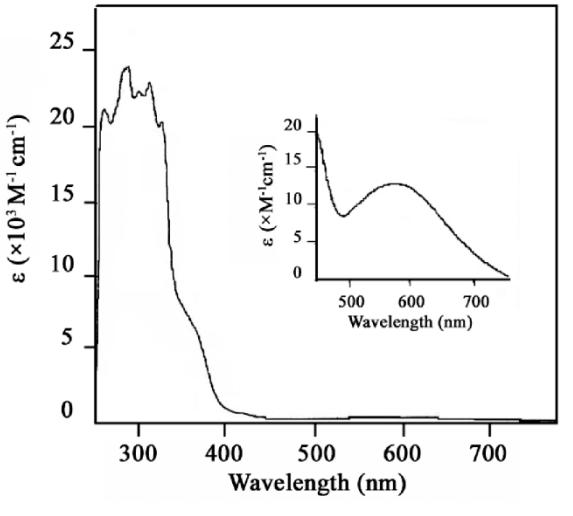

Figure 3. Electronic absorption spectrum of **1** in DMSO. Inset is the spectrum of **1** in the visible region.

Table 3. Electronic absorption data for **1**, compared to free H_2L and pyridine.

Complex **1**			Free ligands and pyridine (molar ratio 2:1)		
λ (nm)	ε ($M^{-1}cm^{-1}$)	Transition assignment	λ (nm)	ε ($M^{-1}cm^{-1}$)	Transition assignment
259	2.07×10^4	π–π*	258	1.75×10^4	π–π*
291	2.37×10^4	π–π* + LMCT	292	1.37×10^4	π–π*
302	2.24×10^4	LMCT			
317	2.3×10^4	π–π*	317	2.22×10^4	π–π*
332	2.08×10^4	π–π*	332	2.12×10^4	π–π*
371	5.92×10^3	LMCT			
600	5.92×10^2	d–d			

stronger ($\varepsilon = 2.37 \times 10^4\,M^{-1}cm^{-1}$) for **1** than that in the free ligands spectrum ($\varepsilon = 1.37 \times 10^4\,M^{-1}cm^{-1}$). It is thus concluded that both ligands and **1** (~40%) contribute to the spectrum at 291 nm. Absorptions at 302 nm and the shoulder at 371 nm are not observed in the ligand and solvent spectrum. Consequently, they are assigned to LMCT transitions [32, 36, 37]. A summary of transition assignments is listed in table 3.

The electronic spectrum of **1** in the visible region shows a broad, weak absorption band, $\varepsilon = 592\,M^{-1}cm^{-1}$, centred at 600 nm. An estimation using the Tanabe–Sugano energy level diagram [38] for a d^4 ion in an octahedral environment, given that the Racah parameter $B = 1140\,cm^{-1}$ for Mn(III), reveals a Ligand Field Stabilization Energy (LFSE) of $18{,}240\,cm^{-1}$ for **1**, in good agreement with the value of $17{,}900\,cm^{-1}$ for $Mn(acac)_3$ (Hacac = 2,4-pentanedione) [39]. In addition, extinction coefficients for spin-only allowed transitions of six-coordinated complexes of low symmetry are typically 10^2–10^3 [39]. The extinction coefficient for **1**, $\varepsilon = 592\,M^{-1}cm^{-1}$, fits nicely with this description. This implies that **1** remains six-coordinate in solution, with retention of solvent molecules in the coordination sphere. The broad feature of the 600 nm transition is rationalized as being due to the low symmetry (D_{2d}) of **1**, by which the ^5E_g and $^5T_{2g}$ terms of free Mn(III) split into $^5A_1 + {}^5B_1$ and $^5B_2 + {}^5E$ terms, respectively. Similar transition probabilities contribute to the broadness of the absorption band at 600 nm. Although solvent molecules probably remain coordinated to the Mn(III) ion in solution, the coordination sphere is labile as indicted by long bond lengths in the solid state. Since **1** is aimed at producing superoxide reactivity, lability of solvent coordination is an advantage for superoxide binding.

3.3. *Reaction of 1 with superoxide*

3.3.1. Inhibition of pyrogallol autoxidation. Pyrogallol autoxidation generates a variety of intermediates, including superoxide, that can be monitored at 318 nm. It has been shown that autoxidation is inhibited if superoxide formation is quenched, for example in the presence of SOD, and this has been used to assay SOD-like activity [26, 27]. SOD-like activity of **1** was evaluated by measuring inhibition of pyrogallol autoxidation. Kinetics of pyrogallol autoxidation showed a linear increase of absorption at 318 nm with time (figure 4, inset) in the presence of 30 μM pyrogallol. The autoxidation rate, V_o, was determined to be $1.71 \times 10^{-3}\,s^{-1}$. Autoxidation slowed in the presence of **1**. The reaction rate in the presence of **1**, V_t, was also measured

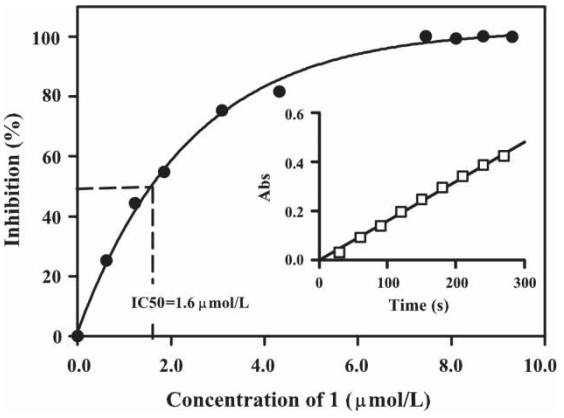

Figure 4. Inhibition of pyrogallol autoxidation in the presence of **1**. Inhibition, I (%), is calculated as mentioned in the text. Inset shows pyrogallol autoxidation rate, measured in absorption units ($\lambda = 318$ nm) vs. time in seconds, mediated by Tris-HCl buffer (50 mM, pH 8.2).

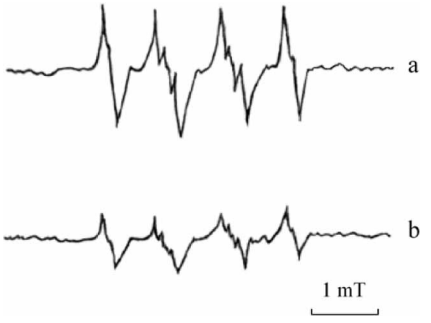

Figure 5. EPR spectra of spin adduct DMPO–$O_2^{\bullet-}$ radical (a) generated by K_2O and DMPO in DMSO solution, (b) as for (a) but in the presence of **1** (1.5 μM).

with varying concentration of **1**. Inhibition, I, can then be calculated according to the equation $I = (V_o - V_t)/V_o$. Figure 4 depicts inhibition against concentration of **1**. The concentration of **1** at which the autoxidation of pyrogallol is inhibited by 50%, IC50, was 1.6×10^{-6} M.

3.3.2. Spin trapping EPR. In order to obtain further evidence that **1** shows reactivity with $O_2^{\bullet-}$, a spin trap experiment was performed, where KO_2 was used as the radical source. In the presence of the spin trap DMPO any existing free $O_2^{\bullet-}$ will be rapidly captured to form DMPO–$O_2^{\bullet-}$, which displays a characteristic EPR signal [28–31]. The reactivity of **1** with $O_2^{\bullet-}$ could be elucidated by comparison of the signal amplitude in EPR spectra recorded in the absence and presence of **1**. In a solution that contains merely KO_2 (14.1 μM) and DMPO (1.5 mM) a well-structured EPR spectrum was observed (figure 5a). This consists of four main lines, each exhibiting hyperfine structure. These features are recognized as originating from DMPO–$O_2^{\bullet-}$ [28–31].

When the EPR spectrum was recorded in a sample where **1** (1.5 μM) was first added to a solution containing KO_2 (14.1 μM) followed by the addition of DMPO (1.5 mM) in order to capture any remaining $O_2^{\bullet-}$, a similar DMPO–$O_2^{\bullet-}$ EPR signal (figure 5b),

but with dramatically reduced signal intensity, was obtained. Signal intensity is inversely correlated to the concentration of **1** added (not shown). These results indicate clearly that the presence of **1** inhibits the formation of DMPO–$O_2^{\bullet-}$, and thus implies reactivity of **1** with superoxide. Using signal intensities in the absence (I_0^{epr}) and presence (I^{epr}) of **1** as probe, the reaction activity of **1** with superoxide radical anion can be determined in terms of inhibition of DMPO–$O_2^{\bullet-}$ formation. The inhibition, I, can be expressed as $I=(I_0^{epr}-I^{epr})/I_0^{epr}$. The IC50 value determined in this way is $\sim 1.2\times 10^{-6}$ M and is close to the value deduced from the inhibition of pyrogallol autoxidation. It is also comparable with other MnSOD-mimicking complexes reported in the literature [34, 35, 40, 41].

In order to prove that only DMPO–$O_2^{\bullet-}$ gives rise to the EPR spectrum a series of control experiments were carried out, recording EPR spectra of KO_2 only, complex **1** only, KO_2 plus **1** and **1** plus DMPO. No combination showed any EPR signal. It was therefore concluded that only DMPO–$O_2^{\bullet-}$ contributes to the spectra in figure 5 and that the signal is diminished in the presence of **1**. In addition, the possibility of a reaction between DMPO–$O_2^{\bullet-}$ and **1** was examined. The EPR spectrum was compared with that shown in figure 5(a), and no change was observed. Thus there is no reaction between DMPO–$O_2^{\bullet-}$ and **1** under the experimental conditions employed.

It has been established that the reaction of SOD and synthetic metal systems that have SOD-like activity [42] involves a two-step reaction:

$$M_{ox} + O_2^{\bullet-} \rightarrow M_{red} + O_2$$
$$M_{red} + O_2^{\bullet-} + 2H^+ \rightarrow M_{ox} + H_2O_2$$

In the experiments, both inhibition of pyrogallol autoxidation and diminished DMPO–$O_2^{\bullet-}$ formation in the presence of **1** provide clear evidence that the former reaction takes place. From a thermodynamic point of view, both reactions are feasible. The Gibbs free energy change (ΔG) for the former reaction is $-9.7\,kJ\,mol^{-1}$ using redox potentials $E^\circ(O_2/O_2^{\bullet-})=-0.5\,V$ (*versus* NHE) in DMSO [43, 44] and E°[Mn(III)/Mn(II)] = $+0.6\,V$ (obtained from preliminary measurements, not shown); ΔG of the latter reaction is $-143.8\,kJ\,mol^{-1}$, taking $E^\circ(O_2^{\bullet-},\ 2H^+/H_2O_2)=+0.89\,V$ [43, 44]. These negative ΔG values indicate that both reactions are thermodynamically favoured.

Although direct evidence for the latter reaction is not to hand, it is noted that the former alone would lead to an EPR-visible Mn(II) species. By inspection of the EPR spectrum recorded after allowing reaction between **1** and $O_2^{\bullet-}$ (see e.g. figure 5b), no Mn(II) signal was found. This is taken as an indirect indication that any Mn(II) formed was probably reoxidized rapidly through the latter reaction. It is thus suggested that **1** undergoes a cyclic reaction showing SOD-like activity.

In **1** the coordination of solvent molecules is somewhat labile as judged from bond lengths (see earlier). It is proposed that this lability allows the superoxide radical anion to replace one of the coordinating solvent molecules. Comparison between the methanol and the pyridine moieties with consideration of bond length and coordinating properties suggests that methanol is probably more labile than pyridine. A suggested sequence of reactions is shown in figure 6. Loss of methanol seems necessary for the catalytic properties of **1**. It not only provides a binding site for superoxide but also resembles the 5-6-5 mechanism suggested by Lah *et al.* [19] for native FeSOD and MnSOD enzymes. Moreover, this hypothesis consequently implies that the central

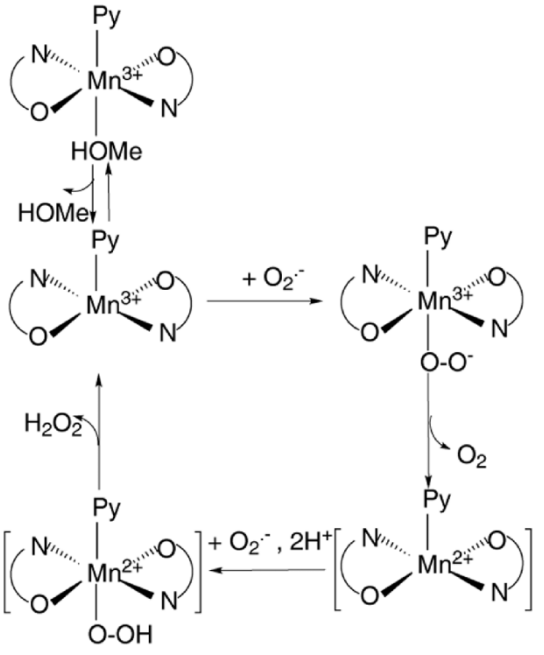

Figure 6. Proposed superoxide dismutation reaction mechanism for **1**.

Mn ion has an N_3O_2 ligand sphere after loss of methanol and an N_3O_3 ligand set upon superoxide addition, resembling the mechanism for native MnSOD. However, the option that the pyridine site can accommodate superoxide cannot be excluded. The outer-sphere H-bonding network in **1** is another interesting feature that shares some similarities with native enzymes. It has been hypothesized that the H-bonding network in native MnSOD functions as a proton funnel [20–22]. It is not entirely clear that H-bonding in **1** is important with respect to its catalytic properties. A reasonable speculation, however, is that H-bonds in **1** might play a role as a proton pool that accommodates and delivers protons that are involved in superoxide dismutation.

Acknowledgements

The work was supported by the National Natural Science Foundation of China (30128003, 20473098 and 20175032). Authors WS, SS and PH express their thanks to the Swedish Energy Agency and DESS for financial support and to the Swedish Consortium for Artificial Photosynthesis for access to technical facilities. PH thanks the Swedish Stiftelsen Bengt Lundqvists Minne for financial support.

References

[1] A.E.G. Cass. In *Metalloproteins*, P.M. Harrison (Ed.), Vol. 1, pp. 121–156, Verlag Chemie, Basel (1985).
[2] J.M. McCord, I. Fridovich. In *Proceedings EMBO Workshop*, A.M. Michelson, J.M. McCord, I. Fridovich (Eds), pp. 1–10, Academic Press, London (1977).

[3] R.H. Weiss, D.P. Riley. *Drugs Future*, **21**, 383 (1996).
[4] J. Pincemail, J. Lecomte, J.-P. Castiau, E. Collard, T. Vasankari, J.-P. Cheramy-Bien, R. Limet, J.-O. Defraigne. *Free Radical Biol. Med.*, **28**, 559 (2000).
[5] R.H. Holm, P. Kennepohl, E.I. Solomon. *Chem. Rev.*, **96**, 2239 (1996).
[6] S.J. Lippard, J.M. Berg. *Principles of Bioinorganic Chemistry*, University Science Books, Mill Valley, California (1994).
[7] I. Fridovich. *J. Exp. Biol.*, **201**, 1203 (1998).
[8] D.P. Riley. *Chem Rev.*, **99**, 2573 (1999).
[9] R.H. Weiss, A.G. Flickinger, W.J. Rivers, M.M. Hardy, K.W. Aston, U.S. Ryan, D.P. Riley. *J. Biol. Chem.*, **268**, 23049 (1993).
[10] R.F. Pasternack, H. Lee, P. Malek, C. Spencer. *J. Inorg. Nucl. Chem.*, **39**, 1865 (1977).
[11] R.F. Pasternack, B. Halliwell. *J. Am. Chem. Soc.*, **101**, 1026 (1979).
[12] R.F. Pasternack, W.R. Stowronek. *J. Inorg. Biochem.*, **11**, 261 (1979).
[13] R.F. Pasternack, A. Banth, J.M. Pasternack, C.S. Johnson. *J. Inorg. Biochem.*, **15**, 261 (1981).
[14] J.R. Sorenson. *J. Prog. Med. Chem.*, **26**, 437 (1989).
[15] G.E. Borgstahl, H.E. Parge, M.J. Hickey, W.F. Beyer, Jr, R.A. Hallewell, J.A. Tainer. *Cell*, **71**, 107 (1992).
[16] R.A. Edwards, M.M. Whittaker, J.W. Whittaker, G.B. Jameson, E.N. Baker. *J. Am. Chem. Soc.*, **120**, 9684 (1998).
[17] M.L. Ludwig, A.L. Metzger, K.A. Pattridge, W.C. Stallings. *J. Mol. Biol.*, **219**, 335 (1991).
[18] M.W. Paker, C.C. Blake. *J. Mol. Biol.*, **99**, 649 (1988).
[19] M.S. Lah, M.M. Dixon, K.A. Pattridge, W.C. Stallings, J.A. Fee, M.L. Ludwig. *Biochemistry*, **34**, 1646 (1995).
[20] Y. Hsieh, Y. Guan, C. Tu, P.J. Bratt, A. Angerhofer, J.R. Lepock, M.J., Hickey, J.A. Tainer, H.S. Nick, D.N. Silverman. *Biochemistry*, **37**, 4731 (1998).
[21] Y. Guan, M.J. Hickey, G.E. Borgstahl, R.A. Hallewell, J.R. Lopock, D. O'Connor, Y. Hsieh, H.S. Nick, D.N. Silverman, J.A. Tainer. *Biochemistry*, **37**, 4722 (1998).
[22] C.A. Ramilo, V. Leveque, Y. Guan, J.R. Lopock, J.A. Tainer, H.S. Nick, D.N. Silverman. *J. Biol. Chem.*, **274**, 27711 (1999).
[23] T. Sala, M.V. Sargent. *J. Chem. Soc., Chem. Comm.*, **6**, 253 (1978).
[24] A.W. Addison, P.J. Burke. *J. Heterocycl. Chem.*, **18**, 803 (1981).
[25] G.M. Sheldrick. *SHELXL97 and SHELXS97*, University of Göttingen, Germany (1997).
[26] S. Marklund, G. Marklund. *Eur. J. Biochem.*, **47**, 469 (1974).
[27] G.L. Zou, X.F. Gui, X.L. Zhong, R.F. Zhu. *Prog. Biochem. Biophys.*, **4**, 71 (1986).
[28] C.N. Guo, J.F. Xiang, J. Feng, Y.L. Tang, C.P. Chen, G.Z. Xu. *J. Colloid. Interface Sci.*, **246**, 401 (2002).
[29] C.P. Chen, R.P. Veregin, J.R. Harbour, M.L. Hair, S.L. Issler, J. Tramp. *J. Phys. Chem.*, **93**, 2607 (1989).
[30] C.P. Chen, B.M. Zhou, D.H. Lu, G.Z. Xu. *J. Photochem. Photobiol. A: Chem.*, **89**, 25 (1995).
[31] C.P. Chen, B.M. Zhou, D.H. Lu, G.Z. Xu. *J. Photogra. Sci.*, **43**, 134 (1995).
[32] A. Neves, S.M. Erthal, I. Vencato, A.S. Ceccato. *Inorg. Chem.*, **31**, 4749 (1992).
[33] J.W. Whittaker, M.M. Whittaker. *J. Am. Chem. Soc.*, **113**, 5528 (1991).
[34] N. Kitajima, M. Osawa, N. Tamura, Y. Moro-Oka, T. Hirano, M. Hirobe, T. Nagano. *Inorg. Chem.*, **32**, 1879 (1993).
[35] R. Rajan, R. Rajaram, B.U. Nair, T. Ramasami, S.K. Mandal. *J. Chem. Soc., Dalton Trans.*, **9**, 2019 (1996).
[36] A. Panja, N. Shaikh, S. Gupta, R. Butcher, P. Banerjee. *Eur. J. Inorg. Chem.*, **8**, 1540 (2003).
[37] X. Li, V.L. Pecoraro. *Inorg. Chem.*, **28**, 3403 (1989).
[38] F.A. Cotton. *Chemical Applications of Group Theory*, 3rd Edn, Wiley, New York (1990).
[39] A.B.P. Lever. *Inorganic Electronic Spectroscopy*, 2nd Edn, Elsevier, New York (1986).
[40] M. Baudry, S. Etienne, A. Bruce, M. Palucki, E. Jacobson, B. Malfroy. *Biochem. Biophys. Res. Commun.*, **192**, 964 (1993).
[41] D.P. Riley, R.H. Weiss. *J. Am. Chem. Soc.*, **116**, 387 (1994).
[42] A.M. Michelson, J.M. McCord, I. Fridivich (Eds). *Superoxide and Superoxide Dismutases*, Academic Press, London (1977).
[43] J.R. Harbour, M.L. Hair. *Adv. Colloid. Interfac. Sci.*, **24**, 103 (1986).
[44] W.M. Latimer (Ed.). *Oxidation Potentials*, Prentice-Hall, New York (1953).